agriculture

MDPI

*Article*

# Effect of Ultrasound-Assisted Vacuum Far-Infrared on the Drying Characteristics and Qualities Attributes of Cistanche Slices

**Bowen Wu, Guojun Ma, Fangxin Wan, Junmin Ma, Zepeng Zang, Yanrui Xu, Ao Chen and Xiaopeng Huang ***

College of Mechanical and Electrical Engineering, Gansu Agricultural University, Lanzhou 730070, China; wubw@st.gsau.edu.cn (B.W.); magj@gsau.edu.cn (G.M.); wanfx@gsau.edu.cn (F.W.); majm@gsau.edu.cn (J.M.); zangzp@st.gsau.edu.cn (Z.Z.); xuyanr@st.gsau.edu.cn (Y.X.); chenao@st.gsau.edu.cn (A.C.)
* Correspondence: huangxp@gsau.edu.cn; Tel.: +86-138-9315-9327

**Abstract:** This study applied direct-contact ultrasound-assisted Vacuum Far-Infrared (VFIR) to dry Cistanche slices, investigating the influence of radiation temperature (45 °C, 55 °C, 65 °C), ultrasonic frequency (20 kHz, 40 kHz, 60 kHz) and ultrasonic power (72 W, 96 W, 120 W) on the physicochemical properties, drying characteristics, and microstructure of Cistanche slices. The results showed that the application of ultrasound had a significant enhancement effect on the drying process, with drying time decreasing as radiation temperature, ultrasonic power, and ultrasonic frequency increased. The drying rate curves under three experimental factors exhibited a brief acceleration stage followed by a deceleration stage. Under different drying conditions, the contents of Iridoid and phenylethanoid glycosides in dried products were higher than those under natural drying (ND). Specifically, the content of catalpol at 55 °C, 96 W, 40 kHz (0.56 mg/g) and the content of Leonuride at 55 °C, 96 W, 60 kHz (0.67 mg/g) increased by 1.81 and 1.9 times, compared to ND. The rest of the nutrient content and antioxidant activity increased with the increase in ultrasonic frequency. Compared to ND, ultrasonic-assisted VFIR drying improved the color and rehydration capacity of dried products. Observation of the microstructure revealed that the application of ultrasound made the interior of Cistanche slices loose and porous. In summary, ultrasonic-assisted VFIR drying not only enhances the drying rate but also improves the quality of dried products.

**Keywords:** direct-contact ultrasound; intensify; cistanche drying; microstructure; physicochemical quality

check for updates

**Citation:** Wu, B.; Ma, G.; Wan, F.; Ma, J.; Zang, Z.; Xu, Y.; Chen, A.; Huang, X. Effect of Ultrasound-Assisted Vacuum Far-Infrared on the Drying Characteristics and Qualities Attributes of Cistanche Slices. *Agriculture* **2024**, *14*, 557. https://doi.org/10.3390/agriculture14040557

Academic Editors: Perla A. Gómez and Isabel Lara

Received: 28 February 2024
Revised: 20 March 2024
Accepted: 28 March 2024
Published: 31 March 2024

**Copyright:** © 2024 by the authors. Licensee MDPI, Basel, Switzerland. This article is an open access article distributed under the terms and conditions of the Creative Commons Attribution (CC BY) license (https://creativecommons.org/licenses/by/4.0/).

## 1. Introduction

Cistanche (*Cistanche deserticola Ma*), belonging to the Orobanchaceae, is a perennial parasitic herbaceous plant and a precious medicinal material. It found its primary cultivation in the tropical and subtropical belts of China, Iran, India, and Mongolia. [1,2]. Due to its rich bioactive ingredients, it is known as the "desert ginseng" [3] and is often processed into capsules, wine, tea, and other health products to enter the health food market [4]. Studies have shown that Cistanche has anti-aging, anti-fatigue [5], anti-inflammatory [6], and analgesic effects. However, fresh Cistanche has relatively high moisture and sugar content, making it prone to softening and rot. In order to prolong the shelf life and improve its economic benefits, it is usually subjected to dehydration processing [7]. Natural drying is the traditional drying method for Cistanche, but it is highly dependent on weather conditions, and the quality of the dried product is difficult to guarantee. Moreover, prolonged natural drying not only causes enzymatic hydrolysis of polyphenol oxidase and browning of the flesh but also leads to significant loss of effective ingredients such as phenylethanoid glycosides, severely affecting the medicinal and economic value of dried Cistanche products [8].

Far-Infrared (FIR) radiation is a form of radiation heating technology that provides consistent heat and mass transfer direction. When the energy released by the infrared heat source penetrates the surface of the material, it heats both the surface and the interior of the material simultaneously, achieving uniform heating and rapid dehydration. Consequently,

FIR drying offers the benefits of even heating, increased drying efficacy, reduced energy usage, and superior product quality [9,10]. The depth of penetration depends on the thickness of the product, the activity of the water and the composition of the product. The results of Deepika et al. [11] indicated that FIR is ideal for thin-layer drying. Vacuum far-infrared drying (VFIR) technology employs infrared radiation for heating materials within a vacuum setting. The addition of a vacuum effectively prevents thermal and oxidative damage to active substances within the materials under sub-atmospheric pressure, reduces the loss of heat-sensitive nutrients, lowers the boiling point of water, thereby enhancing heat transfer rates more effectively [12,13], and thus is widely used in food drying. In recent years VFIR drying technology has been reported in the processing of agricultural products such as apples [14], and lemons [15]. Nonetheless, although VFIR plays a substantial role in facilitating heat transfer throughout the drying process, its capacity to stimulate mass transfer remains limited. [16]. Hence, there is a need to employ efficient techniques for enhancing mass transfer in order to improve dehydration rates and product quality.

Ultrasound, as a non-thermal processing technique, has been widely applied in food drying in recent years. Ultrasound is an elastic mechanical wave that can propagate in gas, liquid, and solid, with strong penetration and vibration characteristics [17]. When ultrasound energy is transmitted into the interior of the material, the material undergoes continuous mechanical pressure due to the high-frequency vibration it generates, reducing the adhesion force of moisture attached to the capillaries inside. This facilitates the flow and diffusion of moisture, promoting mass transfer within the material [18]. Ultrasound technology exists in three forms: ultrasound pretreatment, gas-coupled ultrasound, and direct-contact ultrasound. Among them, gas-coupled ultrasound, as a method of ultrasound enhancement, can significantly shorten drying time [19]. However, it suffers from large energy attenuation and minimal effect on mass transfer, leading to excessive energy consumption. Direct-contact ultrasound involves placing the material directly on an ultrasound radiation plate, where ultrasound energy is transmitted directly into the material without passing through a gas medium. This method effectively increases the internal mass transfer rate of the material, reduces ultrasound energy attenuation, and improves energy utilization. Feng et al. [20] investigated the effects of combined direct-contact ultrasound and FIR drying on the drying characteristics and quality of ginger. They found that employing ultrasound notably decreased drying time expedited the movement of free water, and elevated both antioxidant activity and nutrient levels. Yang et al. [21] investigated the water migration and microstructure of taro during direct-contact ultrasound-enhanced FIR radiation drying, and the results showed that the use of direct-contact ultrasound not only accelerated the drying process of taro but also improved its porosity.

This study applied direct contact ultrasonic technology to VFIR drying of Cistanche slices, investigating the effects of different drying temperatures, ultrasonic power, and ultrasonic frequency on the drying characteristics of Cistanche slices, and evaluating changes in their quality (Total phenol, total flavonoid and polysaccharide contents, antioxidant capacity, rehydration ratio and color value) and microstructure.

## 2. Materials and Methods

### *2.1. Experimental Materials*

Fresh Cistanche was harvested in February 2023 in Jinta County, Jiuquan City, Gansu Province, China. After cleaning, the Cistanche was immediately placed in a constant temperature and humidity chamber and refrigerated at 2–4 °C. The average water content of Cistanche was measured according to the official method of AOAC as 72.7%. Cistanche specimens without surface damage, uniform thickness, and intact appearance were selected as raw materials. One hour before the experiment, the Cistanche was placed at room temperature (22 ± 1 °C). After washing and draining, the Cistanche was peeled and sliced to a thickness of 5 mm. Each group of samples weighed 120 ± 0.5 g.

### 2.2. Instrument and Equipment

The structure and parameters of the VFIR drying equipment utilized in this experiment are detailed in reference [22]. Three custom ultrasonic generators were used, with frequencies of 20 kHz, 40 kHz, and 60 kHz, all rated at 600 W (Shenzhen Baist Ultrasound Technology Co., Ltd., Shenzhen, China).

### 2.3. Experimental Methods

In this experiment, ultrasonic-assisted VFIR drying technology was used to dry Cistanche slices. Based on the results of preliminary trials, radiation temperature (45 °C, 55 °C, 65 °C), ultrasonic power (72 W, 96 W, 120 W), and ultrasonic frequency (20 kHz, 40 kHz, 60 kHz) were selected as experimental factors for single-factor orthogonal experimental design. The specific experimental design can be found in Table 1. The specific experimental design can be found in Table 1. Before the experiment, the equipment was preheated for 10 min to the predetermined parameters. The pre-weighed Cistanche slices were evenly spread on the vibrating plate for drying. The samples were weighed every 30 min until the moisture content reached below 10% (wb) [23], with each experimental group repeated 3 times.

**Table 1.** Single-factor experimental design of ultrasonic-assisted VFIR drying.

| Experiments Number | Radiation Temperature (°C) | Ultrasonic Power (W) | Ultrasonic Frequency (kHz) |
|---|---|---|---|
| 1 (ND) | —— | —— | —— |
| 2 | 55 | —— | —— |
| 3 | 45 | 96 | 40 |
| 4 | 55 | 96 | 40 |
| 5 | 65 | 96 | 40 |
| 6 | 55 | 72 | 40 |
| 7 | 55 | 120 | 40 |
| 8 | 55 | 96 | 20 |
| 9 | 55 | 96 | 60 |

The control experiments include natural drying (ND) and VFIR drying. For ND: Place the samples outdoors and expose them to sunlight. Lay the 5 mm thick slices of Cistanche slices evenly on drying trays, and record the weight of Cistanche slices every 3 days until the moisture content decreases to below 10% (wb). For VFIR drying: Dry the samples at a radiation temperature of 55 °C. Weigh the samples every 30 min until the moisture content reaches below 10% (wb).

### 2.4. Drying Characteristics

#### 2.4.1. Dry Basis Moisture Content

The moisture content of the dried base in the drying process of the Cistanche was calculated as follows:

$$M_t = \frac{W_t - W_d}{W_d} \quad (1)$$

where $M_t$ is the dry basis moisture content of Cistanche slices at time t (%), $W_t$ is the mass of Cistanche slices at time t (g), $W_d$ is the mass of dry matter in Cistanche slices (g).

#### 2.4.2. Moisture Ratio

The moisture ratio of the Cistanche slices during drying was calculated as follows:

$$MR = \frac{M_t - M_f}{M_i - M_f} \quad (2)$$

where $MR$ is the moisture ratio of Cistanche slices, $M_i$ is the initial moisture content of Cistanche slices (%), and $M_f$ is the equilibrium moisture content of Cistanche slices (%).

Due to the extremely low equilibrium moisture content of Cistanche slices, the Equation of the *MR* of Cistanche slices at different drying times is simplified as Equation (3):

$$MR = \frac{M_t}{M_i} \tag{3}$$

2.4.3. Average Drying Rate

The average drying rate of the Cistanche slices during drying was calculated as follows:

$$DR = \frac{M_{t2} - M_{t1}}{t_2 - t_1} \tag{4}$$

where $DR$ is the average drying rate of the Cistanche slices; $M_{t2}$, $M_{t1}$ is the weight of the sliced Cistanche at times $t_2$ and $t_1$ (g), $t_2 - t_1$ is the time interval between two drying processes (min).

*2.5. Quality Attributes*

2.5.1. Total Phenolic Content ($TPC$)

$TPC$ was determined using the Folin-Ciocalteu method, with gallic acid as the standard, based on the method by Beato [24]. Calculate the $TPC$ in Cistanche slices according to Equation (5):

$$TPC = \frac{(C_c \times V_{c2})}{(V_{c1} \times M_c)} \tag{5}$$

where $TPC$ is the total Phenolic content, $C_c$ is the mass concentration of gallic acid (mg/mL), $V_{c1}$ is the volume of the sample extract used during titration (mL), $V_{c2}$ is the volume of the extraction solution (mL), and $M_c$ is the mass of Cistanche slices' dry matter (g).

2.5.2. Total Flavonoid Content ($TFC$)

The $TFC$ in Cistanche slices was assessed utilizing the sodium nitrite-aluminum nitrate-sodium hydroxide method, following the measurement procedure outlined by Lay [25], and employing catechin as the calibration standard. Calculate the $TFC$ in accordance with Equation (6):

$$TFC = \frac{(C_d \times V_{d2})}{(V_{d1} \times M_d)} \tag{6}$$

where $TFC$ is the total flavonoid content, $C_d$ is the mass concentration of catechins (mg/mL), $V_{d1}$ is the volume of the sample extract used during titration (mL), $V_{d2}$ is the volume of the extraction solution (mL), and $M_d$ is the mass of Cistanche slices' dry matter (g).

2.5.3. Polysaccharide Content ($PC$)

The content of Polysaccharides in Cistanche was determined using the phenol-sulfuric acid method, following the method outlined by Dubois [26], with sucrose as the standard for calibration. The $PC$ in Cistanche slices was calculated using Equation (7):

$$PC = \frac{(C_p \times V_{p2})}{(V_{p1} \times M_p)} \tag{7}$$

where $PC$ is the Polysaccharide content, $C_p$ is the mass concentration of polysaccharides (mg/mL), $V_{p1}$ is the volume of the sample extract used during titration (mL), $V_{p2}$ is the volume of the extraction solution (mL), and $M_p$ is the mass of Cistanche slices' dry matter (g).

2.5.4. Antioxidant Properties

The total antioxidant capacity of organic active substances was determined using the DPPH method, following the procedure outlined by Nencini [27]. The antioxidant capacity of the samples was calculated according to Equation (8):

$$IR = \frac{(A_0 - A)}{A} \times 100\% \tag{8}$$

where $IR$ is the inhibition rate of the sample solution (%), $A$ is the absorbance of the sample solution, and $A_0$ represents the absorbance of the solution without the sample.

#### 2.5.5. Phenylethanoid Glycosides and Iridoid

The contents of Phenylethanoid Glycosides and Iridoids in Cistanche were determined by HPLC. The chromatographic conditions were as follows: Agilent Eclipes XDB-B-C-18 (250 mm × 4.6 mm, 5 μm) column, column temperature of 30 °C, volume flow rate of 1.0 mL/min, gradient elution mobile phase of water (A)-acetonitrile (B); 0~6 min, 0~10% B; 6~10 min, 20~25% B; 10~15 min, 25~30% B; 15~20 min, 30~35% B; 20~24 min, 35~65% B; 24~26 min, 65~45% B; 26~28 min, 45~10% B; and detection wavelength of 205 mm. Each experiment was repeated 3 times.

#### 2.5.6. Color Values

The determination of Cistanche's color characteristics was conducted using a handheld colorimeter (CR-410, Konica Minolta, Tokyo, Japan), measuring the $L$, $a$, and $b$ values before and after drying. The total color difference, represented by $\Delta E$, indicates the difference in color between the tested sample and the vibrant color. A smaller $\Delta E$ value suggests a better color for the dried Cistanche product. The $\Delta E$ value is calculated according to Equation (9):

$$\Delta E = \sqrt{(L^* - L_0)^2 + (a^* - a_0)^2 + (b^* - b_0)^2} \quad (9)$$

where $\Delta E$ is the total color difference of Cistanche slices. $L^*$, $a^*$, and $b^*$ are the brightness, red-green, and yellow-blue values of fresh Cistanche slices, respectively. $L_0$, $a_0$, and $b_0$ represent the brightness, red-green, and yellow-blue values of dried Cistanche slices.

#### 2.5.7. Rehydration Ratio ($RR$)

Place 3 g of dried Cistanche slices into a constant temperature water bath at 25 °C, allowing them to soak uniformly for 360 min. Subsequently, transfer them onto clean absorbent paper to remove surface moisture. Next, weigh the samples after Rehydration and compare the weight with the dried sample, repeating the experiment three times for each group. Calculate the $RR$ according to Equation (10):

$$RR = \frac{G_f}{G_g} \quad (10)$$

where $RR$ is the Rehydration Ratio, $Gf$ is the weight of Cistanche slices after removing surface moisture during Rehydration (g), and $Gg$ is the initial weight of the Rehydrated Cistanche slices (g).

#### 2.5.8. Microstructure

Samples of dried products obtained under different drying conditions were prepared into 2 × 2 $mm^2$ specimens, securely affixed to the SEM sample stage using conductive tape. Subsequently, an ion sputter coater was employed to coat the sample surfaces for 90 s. The electron microscope acceleration voltage was set to 5.0 kV, and the samples were observed under the scanning electron microscope at a magnification of 300×. Representative fields were selected for microphotography.

### *2.6. Statistical Analysis*

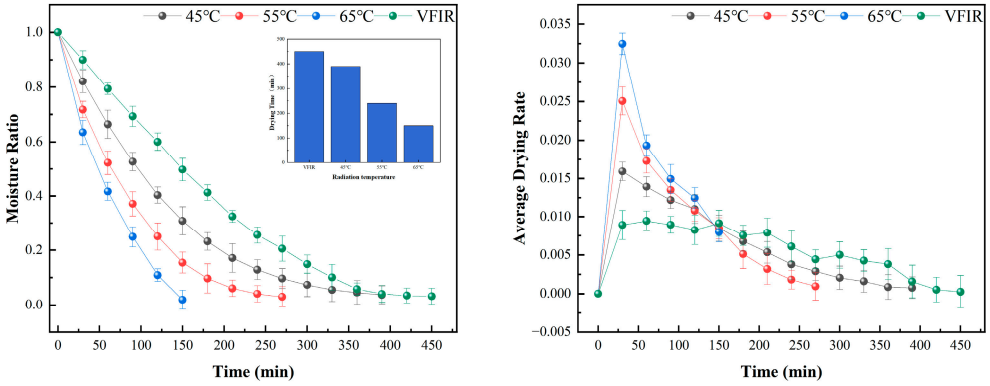
The drying data of Cistanche slices were integrated using Excel 2010 software. Origin 2021 software was employed for graph plotting. Analysis of variance (ANOVA) was conducted using SPSS 24.0.

## 3. Results and Discussion

### *3.1. Drying Characteristics*

#### 3.1.1. Effect of Different Radiation Temperatures on Drying Characteristics

The drying characteristic curves under different radiation temperatures can be seen in Figure 1 (The ultrasonic frequency and ultrasonic power remain constant at 55 °C and 96 W). At radiation temperatures of 45 °C, 55 °C, and 65 °C, the times required for Cistanche slices to dry to below the safe moisture content were 390 min, 240 min, and 150 min. Compared to 45 °C, the drying times at 55 °C and 65 °C were shortened by 38.46% and 61.54%. Observing the drying curves, it can be seen that with the increase in radiation temperature, the moisture content exhibits a decreasing trend, and the drying rate increases with higher temperatures, resulting in shorter drying times. This is because increasing the radiation temperature increases the temperature difference between the material and the drying medium, improving the vapor pressure difference between them, which promotes moisture diffusion and evaporation, thereby accelerating mass transfer, shortening drying time, and increasing drying rate. Additionally, as the radiation temperature increases, Cistanche slices absorb more radiation energy during the drying process, which also increases the drying rate. Furthermore, it was observed that the drying rate curves at different radiation temperatures did not have a clear constant rate stage but mainly concentrated on the falling rate stage. This is because, during drying, the free water content of Cistanche slices continuously decreases, while bound water, due to its association with large molecules such as proteins and polysaccharides, is difficult to remove, resulting in a decrease in drying rate. Initially, the drying rate increases and then decreases, with the drying mechanism shifting to internal diffusion control [28].



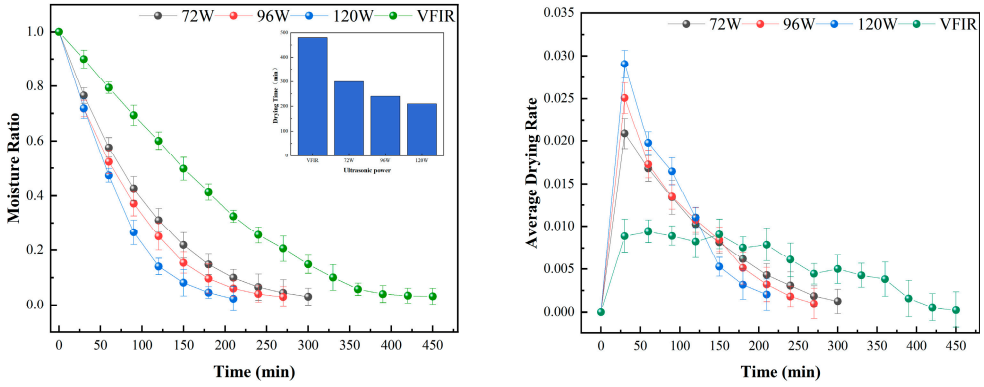

(**a**) (**b**)

**Figure 1.** Effect of different drying temperatures on the drying characteristics of cistanche slices. (**a**) Moisture ratio variation curve, (**b**) Drying rate variation curve.

#### 3.1.2. Effects of Different Ultrasonic Powers on Drying Characteristics

The drying characteristic curves under different ultrasonic powers can be seen in Figure 2 (The radiation temperature and ultrasonic frequency remain constant at 55 °C and 40 kHz). At ultrasonic powers of 72 W, 96 W, and 120 W, the required drying times for Cistanche slices were 300 min, 240 min, and 210 min. By observing the curves, it is evident that ultrasonic power has a significant influence on the drying process. This is because ultrasound causes high-frequency vibrations and turbulence inside Cistanche slices, reducing their ability to adsorb water and enhancing water mobility [29]. Additionally, the compression and expansion caused by ultrasound, known as the "sponge effect", and the formation of micro-jets reduce the thickness of the heat and mass transfer boundary layer, improving the diffusion efficiency inside Cistanche slices and increasing the heat transfer rate [30]. As the ultrasonic power increases, the required drying time further decreases. This is because, with the increase in ultrasonic power, more ultrasonic energy is generated, enhancing the ultrasonic diffusion and mass transfer strengthening effect on

water. Although increasing ultrasonic power can increase the drying rate, the strengthening effect of ultrasound weakens as the moisture content decreases. At the high moisture content stage, due to the high content of free water, ultrasound easily penetrates into the interior of Cistanche slices and propagates therein, which facilitates the propagation of ultrasound. However, as the internal moisture of the sample evaporates and the moisture content decreases, the effect of ultrasound weakens, resulting in a significant decrease in the enhancement effect on moisture diffusion and drying rate [31], manifested as a continuous decrease in drying rate.

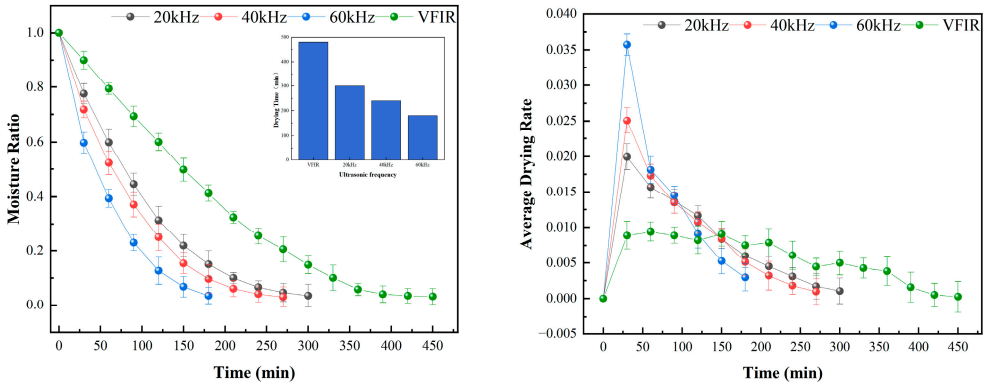



(**a**) (**b**)

**Figure 2.** Effect of different ultrasonic power on the drying characteristics of cistanche slices. (**a**) Moisture ratio variation curve, (**b**) Drying rate variation curve.

3.1.3. Effects of Different Ultrasonic Frequencies on Drying Characteristics

The drying characteristic curves under different ultrasonic frequencies can be seen in Figure 3 (The radiation temperature and ultrasonic power remain constant at 55 °C and 96 W). By observing the curves, it is found that under the 60 kHz frequency, the Cistanche slices require the shortest drying time with the fastest drying rate, which is 27.3% shorter than that under the 20 kHz frequency. With the increase in ultrasonic frequency, the required drying time decreases, and the drying rate increases. When Cistanche slices are placed on the vibrating plate, the radiated ultrasonic energy directly penetrates the interior of the sample, and the propagation of ultrasound exceeds the attraction of liquid molecules, forming numerous microbubbles in the liquid due to cavitation effects. These bubbles are distributed throughout the liquid and undergo implosive collapse when they expand to a critical size [32]. The instantaneous collapse generates extreme temperatures and pressures, which not only significantly accelerate chemical reactions in the surrounding medium but also affect the tightly adsorbed moisture in the capillaries inside the Cistanche slices, facilitating the removal of strongly attached moisture, enhancing the fluidity of microtubes, and accelerating the internal moisture flow rate [33]. Additionally, ultrasound can induce a series of rapid alternating contractions and expansions in solid media, expanding and creating new microchannels, making internal water migration easier [13]. In Figure 3, it is observed that the drying rate curves under different frequencies exhibit a brief acceleration phase followed by a distinct deceleration phase. This is because as the internal moisture of the sample evaporates, the content of free water significantly decreases. This leads to an increase in the internal moisture diffusion resistance of the sample, an increase in the ultrasonic transmission attenuation coefficient, and a decrease in the drying rate [34].




(**a**) (**b**)

**Figure 3.** Effect of different ultrasonic frequencies on the drying characteristics of cistanche slices. (**a**) Moisture ratio variation curve, (**b**) Drying rate variation curve.

### *3.2. Effect of Ultrasound-Assisted VFIR Drying on Quality Attributes of Dried Cistanche Slices*

#### 3.2.1. Total Phenolic Content (*TPC*)

The effect of different drying conditions on *TPC* can be seen in Figure 4a. Under each ultrasonic condition, the *TPC* is higher than that of VFIR drying. The highest *TPC* was 53.18 mg/g, corresponding to a drying condition of 55 °C, 96 W, 60 kHz. As the radiation temperature and ultrasonic power increase, the TPC initially rises and then decreases. Phenolic compounds are a class of thermosensitive substances with antioxidant properties. At lower temperatures, the drying time of the material is longer, leading to significant degradation of phenolic compounds under the action of polyphenol oxidase and peroxidase. With the increase in temperature, the drying time significantly shortened, leading to a corresponding reduction in the time of oxidative reactions and an increase in *TPC*. However, when the temperature is too high, the rapid increase in the degradation rate of phenolic compounds due to high temperatures leads to a decrease in *TPC* [35]. The addition of ultrasound shortened the drying time., thereby reducing the degree of polyphenol degradation. It also breaks covalent bonds, releasing antioxidants, thus increasing the *TPC* of Cistanche slices [36]. However, high-power ultrasound will instead decrease *TPC*. This is because high-intensity ultrasound generates free hydroxyl radicals to degrade polyphenols, damaging phenolic compounds and their antioxidant activity in extracts [37]. With the increase in ultrasonic frequency, the *TPC* continues to increase. Proper ultrasound enhancement can disrupt cell structure [38], causing polymers in the Cistanche cell wall to break down and release more cell wall phenolic compounds or adsorbed phenolic compounds, thereby increasing *TPC*.

#### 3.2.2. Total Flavonoid Content (*TFC*)

The effect of different drying conditions on *TFC* can be seen in Figure 4b. At 55 °C, 96 W, 60 kHz, the *TFC* reached its highest at 59.17 mg/g, which increased by 57.96% compared to the dried product obtained from VFIR drying. When the radiation temperature increased from 55 °C to 65 °C, the *TFC* decreased from 48.00 mg/g to 23.62 mg/g. At lower radiation temperatures, the drying time is longer, leading to continuous degradation reactions of flavonoids in the samples. Increasing the temperature significantly shortens the drying time, inhibits the activity of flavonoid oxidase, facilitates the decomposition of cellular components, releases a large number of flavonoid compounds, and thus preserves the *TFC*. However, excessively high temperatures enhance the activity of flavonoid components and increase the degradation rate, thereby unfavorable for maintaining flavonoid substances [39]. When the ultrasonic power increased to 120 W, the *TFC* decreased to 28.93 mg/g. Although increasing the ultrasonic power enlarges the mass transfer channels of the material, it also enlarges the intercellular gaps [14], accelerating the release of flavonoid substances from the cells. Meanwhile, flavonoid compounds, due to their abun-

dant hydroxyl groups, are easily oxidized, leading to a decrease in the *TFC* in Cistanche slices [40]. With the increase in ultrasonic frequency, *TFC* shows an upward trend. This is because increasing the ultrasound frequency enhances the effect of ultrasound [18], reduces the resistance of moisture outward migration channels in Cistanche slices, shortens drying time, and consequently reduces the oxidation degradation reaction time of flavonoids.

#### 3.2.3. Polysaccharide Content (*PC*)

The effect of different drying conditions on *PC* can be seen in Figure 4c. At 55 °C, 96 W, 40 kHz, the maximum *PC* reached 351.58 mg/g, which represented a 39.12% increase compared to the dried product obtained from VFIR drying. The *PC* showed a trend of first increasing and then decreasing under different radiation temperatures. At 45 °C, the lower drying temperature led to lower drying efficiency, thus increasing the time for polysaccharides to undergo Maillard reaction with free amino acids in the material, resulting in polysaccharide degradation. However, at 65 °C, 96 W, and 40 kHz, the excessively high radiation temperature intensified polysaccharide cleavage into monosaccharides, while accelerating the Maillard reaction rate, leading to a decrease in *PC* [41]. Except for the temperature at 65 °C, the *PC* under other conditions was higher than that of ND. This may be because the addition of ultrasound significantly increased the water solubility of polysaccharides, exposing more hydrophilic groups to hydration due to the disruption of non-covalent intramolecular and intermolecular bonds [42]. Additionally, the sonoporation effect of ultrasound creates pores in the cell membrane, which allows more polysaccharides to be released from the cells. Chemat et al. [32] observed visible cell membrane permeabilization when applying ultrasound to yeast, and obtained higher extraction rates. Furthermore, ultrasound causes degradation of the cell wall and disruption of cell structure, which not only promotes the release of polysaccharides but also increases the accessibility of solvents, thereby enhancing the *PC*. When the ultrasonic power increased to 55 °C, 120 W, 40 kHz, *PC* decreased to 260.27 mg/g, which was because the high ultrasonic power induced more intense mechanical effects, causing the destruction of Cistanche cells, ultimately leading to a decrease in *PC* [43]. As the frequency increased, the *PC* first increased and then slightly decreased. Studies by Chen et al. [44] showed that increasing the ultrasonic frequency can effectively improve the cavitation, thermal, and mechanical effects of ultrasound, enhancing the diffusion rate of solvents and accelerating the dissolution of polysaccharides, thereby increasing the extraction rate of polysaccharides.

#### 3.2.4. Antioxidant Capacity

The effect of different drying conditions on antioxidant capacity can be seen in Figure 4d. The antioxidant capacity is represented by inhibition rate (*IR*), with higher *IR* indicating stronger antioxidant capacity. Niwa et al. [45] demonstrated that FIR radiation can break covalent bonds, releasing antioxidants such as flavonoids, carotenoids, tannic acid, ascorbic acid, albumin, or polyphenols from polymers, thereby enhancing antioxidant activity. The lowest *IR* was 34.92% at 65 °C, 96 W, 40 kHz. As the radiation temperature and ultrasonic power increased, the *IR* first increased and then decreased. Firstly, the increase in radiation temperature altered the structure and content of some monophenolic and flavonoid compounds in Cistanche slices, enhancing their ability to scavenge free radicals [22]. However, excessively high temperatures cause degradation of antioxidants, leading to a decrease in antioxidant capacity. Secondly, ultrasonic cavitation causes microbubbles to implode or collapse, resulting in local increases in temperature and pressure, thereby reducing antioxidant capacity [46]. As the ultrasonic frequency increased, the *IR* significantly increased, which may be because the application of ultrasound can increase the hydroxyl group content, enhancing antioxidant capacity [47]. Additionally, it was observed that the change trend of antioxidant capacity was similar to that of *TPC*. This is because phenolic compounds, as the most active antioxidant derivatives in plants, are considered antioxidants [48]. Other studies have also reported a highly positive correlation between phenolic compounds and antioxidant activity [49].

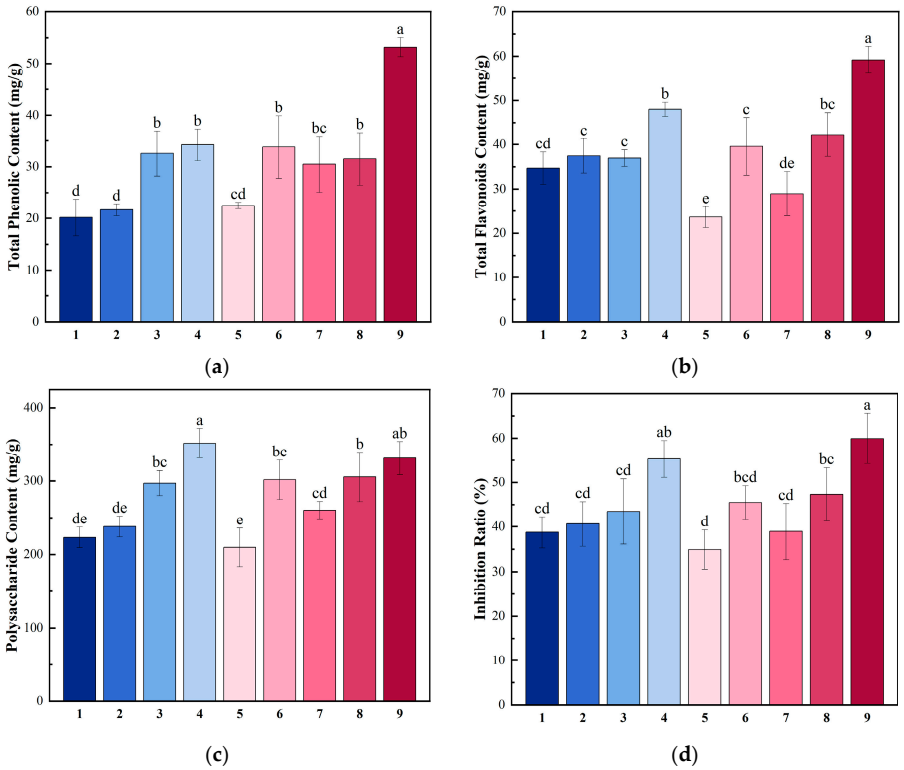



**Figure 4.** Antioxidant properties, *PC*, *TPC*, and *TFC* of Cistanche slices under different drying conditions. (**a**) *TPC*, (**b**) *TFC*, (**c**) *PC*, (**d**) *IR*.

### 3.2.5. Phenylethanoid Glycosides and Iridoid

Phenylethanoid glycoside is one of the most researched types of active compounds in Cistanche currently. As a major active ingredient of Cistanche, it has positive effects such as antioxidation, liver protection, myocardial protection, neuron protection, and memory enhancement [50]. Iridoid is also one of the main chemical components of Cistanche, exhibiting antibacterial, anti-inflammatory, and analgesic effects [43]. The changes in Iridoid and Phenylethanoid glycoside components in Cistanche slices under different drying conditions can be seen in Figure 5. It can be observed that the content of Iridoid and Phenylethanoid glycosides in the dried products obtained by ultrasonic-assisted VFIR drying is higher than that of ND. The maximum contents of Catapol, Leonurusoside, Rhodioloside, Echinacoside, Poliumoside, Verbascoside and Isoacteoside increased by 47.84%, 47.47%, 37.06%, 34.62%, 24.2%, 26.43% and 32.49%, respectively, compared to ND. Except for slightly lower levels of Rhodioloside and Isoacteoside under certain conditions, the rest of the active ingredients in the dried products obtained from ultrasonic-assisted VFIR drying are higher than those in VFIR drying. Since these two types of components are extremely sensitive to light and heat, when the radiation temperature increases from 55 °C to 65 °C, the high-temperature environment causes severe damage to the cell materials. The content of Phenylethanoid glycosides such as Poliumoside, Isoacteoside, Leonurusoside, and Catalpol decreased by 11.43%, 13.1%, 32.12%, and 28.7%. The slight decrease in Verbascoside and Echinacoside content is mainly due to the high temperature damaging the hydrolytic enzymes, preventing the conversion of Echinacoside to Verbascoside [51,52]. Secondly, because Verbascoside and Isoacteoside are structural isomers, the increase in radiation temperature promotes the conversion of Isoacteoside to Verbascoside. When the ultrasonic power increased from 96 W to 120 W, the content of Poliumoside, Isoacteoside, Echinacoside, Leonurusoside, and Catalpol decreased by 11.12%, 8.5%, 17.38%, 27.29%, and 23.91%. This may be due to the excessive ultrasonic power and the resulting instantaneous high temperature, which destroyed the molecular structure, resulting in a decrease in content.

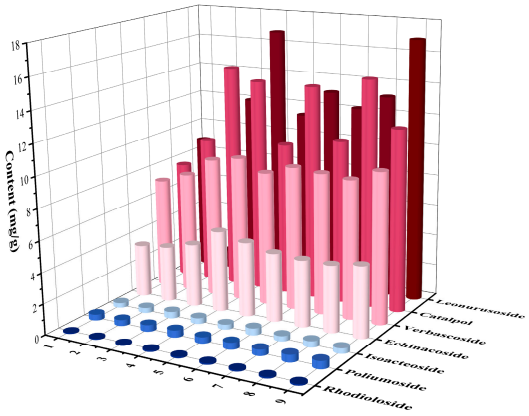



**Figure 5.** Content of Phenylethanol glycoside and Iridoid under different drying conditions.

### 3.2.6. Color Values

The $L^*$, $a^*$, and $b^*$ values of fresh Cistanche are 68.84, 2.51, and 21.58. The changes in color parameters under different drying conditions can be seen in Figure 6. The $\Delta E$ values under different drying conditions are all greater than 5, indicating that ultrasonic-assisted VFIR drying significantly alters the color of Cistanche slices. At 55 °C, 96 W, and 60 kHz, the minimum $\Delta E$ value is obtained at 5.28. VFIR drying has the same heat transfer direction as the mass transfer direction, resulting in a shorter drying time and less oxidative browning of the material. Moreover, drying the samples in a vacuum environment reduces the occurrence of browning caused by oxidation. The addition of ultrasound can also slow down the rate of browning reaction and maintain the original color of the sample [16]. The $b^*$ values of the samples after ultrasonic-assisted VFIR drying are all lower than those of the fresh samples, indicating that ultrasound affects the yellowness value of Cistanche slices. With the increase in temperature, the $\Delta E$ initially increases and then decreases. This is because, under low-temperature conditions, excessively long drying times lead to significant damage to the active substances (such as anthocyanins, carotenoids and sugars) in Cistanche, affecting the color. As the temperature increases, the drying time is significantly reduced. The activity of oxidases in the material is also inhibited, reducing the production of melanoidin-like substances and lowering the color difference value. However, excessively high temperatures exacerbate the Maillard reaction, resulting in the production of melanoidin-like substances [53], increasing the degree of browning of the material and raising the color difference value. Additionally, the mechanical action and cavitation effect of ultrasound increases the intercellular space and widens the micropores, causing surface damage to the material [54]. Therefore, the effective contact area between the material and the ultrasonic medium increases, resulting in a change in color.

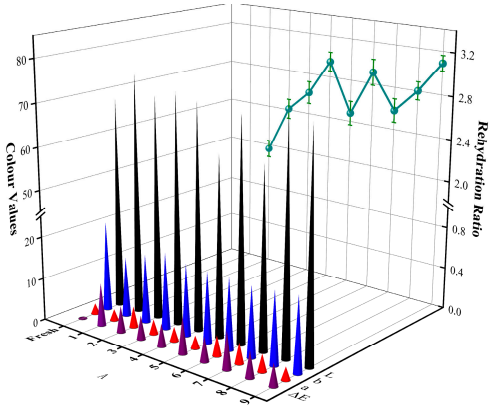


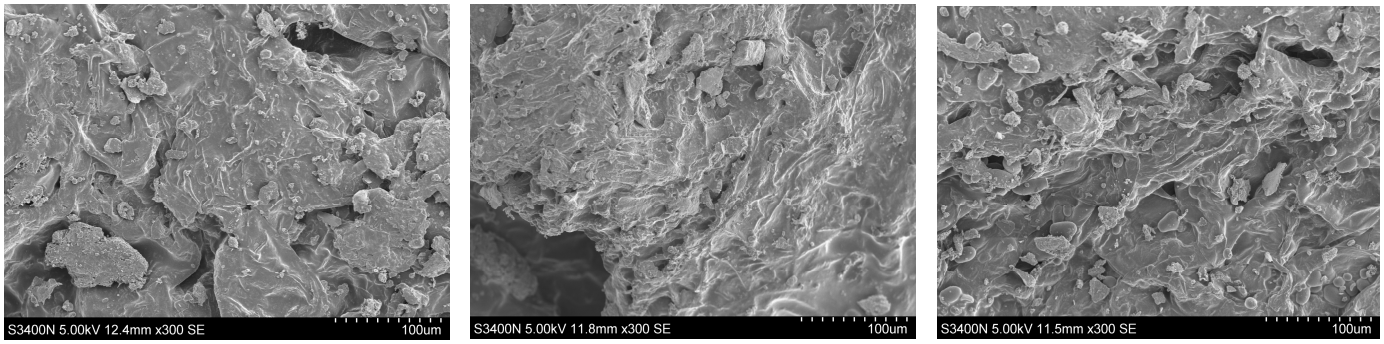

**Figure 6.** Color Values and Rehydration Ratio of cistanche slices under different drying conditions.

3.2.7. Rehydration Ratio (RR)

The RR is an important parameter for measuring the degree of tissue structure damage during the drying process. A higher value indicates less damage to the material's tissue structure and higher integrity [55]. The variations of RR under different drying conditions can be seen in Figure 6. The maximum RR is 3.22, obtained under the conditions of 55 °C, 96 W, and 60 kHz. It can be observed that the RR under various conditions is higher than that of ND. This is because the vacuum conditions contribute to the generation of greater internal stress during the drying process, resulting in more pores in the material and enhancing its rehydration capability [56]. With the increase in radiation temperature and ultrasonic power, the RR shows a trend of first increasing and then decreasing. This is because high temperature and excessive ultrasonic power damage the structure of the material, causing surface cells to lose vitality and forming dense tissue, thereby increasing the resistance to internal water flow and reducing rehydration capability. With the increase in ultrasonic frequency, the RR shows an upward trend. In the study by Liu et al. [31] on ultrasound-assisted hot air drying of purple sweet potatoes, they also observed surface damage and collapse of the samples caused by ultrasound, leading to a decreased rehydration capacity. This may be because high-frequency ultrasound can induce stronger cavitation and mechanical effects, widening the pores and microchannels, thereby reducing the resistance to water transfer and enhancing rehydration capability [29].

3.2.8. Microstructure

The microstructure of the material has a significant impact on the mass transfer and quality characteristics during the drying process. The microstructures under different drying conditions can be seen in Figure 7. The surface of Cistanche slices obtained by ND (Figure 7a) is smooth, dense, and contains a small amount of debris. This is because, under ND, continuous shrinkage accompanied by the removal of moisture causes surface hardening. This dense structure reduces the internal water diffusion path, increases the resistance to water diffusion, and ultimately leads to a lower dehydration rate. After the addition of ultrasound, the surface of Cistanche slices becomes loose and porous, indicating the presence of microchannels induced by ultrasound in the tissue, which can accelerate the internal heat and mass transfer and water diffusion of the sample. Starch granules on the surface of the sample were observed to gelatinize [57] under conditions of 55 °C, 120 W, 40 kHz (Figure 7g) and 65 °C, 96 W, 40 kHz (Figure 7e), forming a dense barrier layer adhering to the surface, with cell tissue being disrupted and forming large cavities, accompanied by a significant degree of fracturing. This is because high-temperature conditions cause varying degrees of stress concentration on the Cistanche slices' surface, exacerbating damage to the pore structure [58]. Moreover, excessive ultrasonic power leads to intense compression and expansion of the tissue, with cavitation effects causing significant impact and damage to the tissue structure, resulting in a decrease in its rehydration capacity, which corroborates the previously measured lower rehydration ratio.




(**a**) (**b**) (**c**)

**Figure 7.** *Cont.*

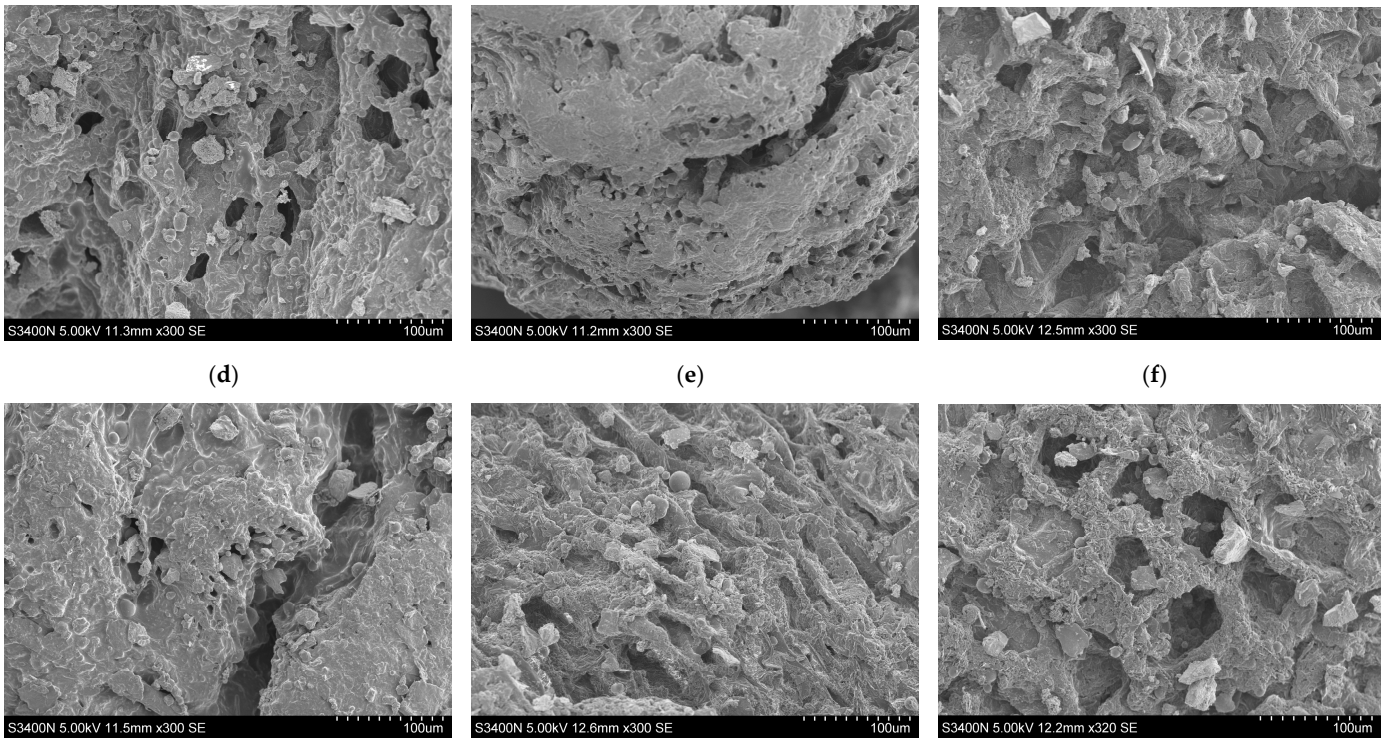



**Figure 7.** Microstructure of cistanche slices under different drying conditions. (**a**) 1, (**b**) 2, (**c**) 3, (**d**) 4, (**e**) 5, (**f**) 6, (**g**) 7, (**h**) 8, (**i**) 9.

## 4. Conclusions

We conducted a study of direct contact ultrasound-assisted VFIR drying of Cistanchis slices by using radiation temperature (45 °C, 55 °C, 65 °C), ultrasonic frequency (20 kHz, 40 kHz, 60 kHz) and ultrasonic power (72 W, 96 W, 120 W) as test factors. It was found that with the increase in radiation temperature, ultrasonic power, and ultrasonic frequency, the drying time could be shortened to varying degrees. The condition with the shortest required drying time is 55 °C, 96 W, 60 kHz. However, during the drying process, as the moisture content of the Cistanche slices decreased, the cavitation and mechanical effects of ultrasound weakened, leading to a significant decrease in the enhancement effect. The drying rate curve showed a brief acceleration stage followed by a deceleration stage, without a clear constant-speed stage. The content of Iridoid and Phenylethanol glycosides in Cistanche-dried products obtained by ultrasonic-assisted VFIR drying was higher than that of ND. The maximum contents of Catapol, Leonurusoside, Rhodioloside, Echinacoside, Poliumoside, Verbascoside and Isoacteoside increased by 47.84%, 47.47%, 37.06%, 34.62%, 24.2%, 26.43% and 32.49%, respectively, compared to ND. The highest *PC* was achieved under the condition of 55 °C, 96 W, 40 kHz, reaching 351.58 mg/g. The maximum values of *TPC*, *TFC*, and antioxidant activity were all achieved under the condition of 55 °C, 96 W, 60 kHz, with values of 53.18 mg/g, 59.17 mg/g, and 59.94%. Quality analysis showed that the increase in ultrasonic frequency significantly improved these qualities. Compared to VFIR drying, ultrasounic-assisted VFIR drying improved the color and rehydration capacity of Cistanche slice-dried products, with a minimum $\Delta E$ value of 5.28 achieved under the condition of 55 °C, 96 W, 60 kHz. However, the improvement in $\Delta E$ was not significant under the condition of high ultrasonic power of 55 °C, 120 W, and 40 kHz. It was observed in the microstructure that with the addition of ultrasound, the interior of the material became loose and porous. However, the gelatinization of starch caused by excessive power and temperature hindered the migration of moisture, reducing the rehydration capacity. By comprehensively considering the drying characteristics and physicochemical qualities, the

optimal drying conditions for Cistanche slices were 55 °C, 96 W, and 60 kHz. Subsequent research will focus on how to support experimentally obtained results with theoretical results, such as theoretical derivations and modeling simulations.

**Author Contributions:** Conceptualization, B.W. and X.H.; methodology, B.W. and Z.Z.; software, B.W. and F.W.; validation, B.W., G.M. and Y.X.; formal analysis, B.W.; investigation, B.W., J.M., F.W. and A.C.; resources, X.H. and F.W.; data curation, B.W. and Y.X.; writing—original draft preparation, B.W.; writing—review and editing, Z.Z. and X.H.; visualization, B.W.; supervision, X.H. and F.W.; project administration, X.H. and G.M.; funding acquisition, X.H. All authors have read and agreed to the published version of the manuscript.

**Funding:** This research was funded by The Gansu Provincial Science and Technology Plan, grant number 23CXNA0017, and was funded by Fangxin Wan.

**Institutional Review Board Statement:** Not applicable.

**Data Availability Statement:** The datasets generated for this study are available upon request from the corresponding author.

**Conflicts of Interest:** The authors declare no conflicts of interest.

## References

1. Wang, X.; Wang, J.; Guan, H.; Xu, R.; Luo, X.; Su, M.; Chang, X.; Tan, W.; Chen, J.; Shi, Y. Comparison of the Chemical Profiles and Antioxidant Activities of Different Parts of Cultivated *Cistanche deserticola* Using Ultra Performance Liquid Chromatography-Quadrupole Time-of-Flight Mass Spectrometry and a 1,1-Diphenyl-2-picrylhydrazyl-Based Assay. *Mol. A J. Synth. Chem. Nat. Prod. Chem.* **2017**, *22*, 2011. [CrossRef]
2. Xu, R.; Chen, J.; Chen, S.; Liu, T.; Zhu, W.; Xu, J. Cistanche deserticola Ma cultivated as a new crop in China. *Genet. Resour. Crop Evol.* **2009**, *56*, 137–142. [CrossRef]
3. Li, Z.; Lin, H.; Gu, L.; Gao, J.; Tzeng, C. Herba Cistanche (Rou Cong-Rong): One of the Best Pharmaceutical Gifts of Traditional Chinese Medicine. *Front. Pharmacol.* **2016**, *7*, 182827. [CrossRef]
4. Luo, Z.; Qing, D.; Sun, Y.; Xu, X.; Zhang, J.; Wang, Z. Development and patent analysis of Cistanche health food. *Northwest Pharm. J.* **2020**, *35*, 940–944.
5. Song, Y.; Zeng, K.; Jiang, Y.; Tu, P. Cistanches Herba, from an endangered species to a big brand of Chinese medicine. *Med. Res. Rev.* **2021**, *41*, 1539–1577. [CrossRef]
6. Zhang, H.; Xiang, Z.; Duan, X.; Jiang, J.; Xing, Y.; Zhu, C.; Song, Q.; Yu, Q.R. Antitumor and anti-inflammatory effects of oligosaccharides from *Cistanche deserticola* extract on spinal cord injury. *Int. J. Biol. Macromol.* **2019**, *124*, 360–367. [CrossRef]
7. Esturk, O. Intermittent and Continuous Microwave-Convective Air-Drying Characteristics of Sage (*Salvia officinalis*) Leaves. *Food Bioprocess Technol.* **2012**, *5*, 1664–1673. [CrossRef]
8. Ai, Z.; Zhang, Y.; Li, X.; Sun, W.; Liu, Y. Widely Targeted Metabolomics Analysis to Reveal Transformation Mechanism of *Cistanche Deserticola* Active Compounds During Steaming and Drying Processes. *Front. Nutr.* **2021**, *8*, 742511. [CrossRef]
9. Kim, W.W.; Ghimeray, A.K.; Wu, J.C.; Eom, S.H.; Lee, B.G.; Kang, W.S.; Cho, D.H. Effect of far infrared drying on antioxidant property, anti-inflammatory activity, and inhibitory activity in A549 cells of Gamguk (*Chrysanthemum indicum* L.) flower. *Food Sci. Biotechnol.* **2012**, *21*, 261–265. [CrossRef]
10. Riadh, M.H.; Ahmad, S.A.; Marhaban, M.H.; Soh, A.C. Infrared Heating in Food Drying: An Overview. *Dry. Technol.* **2015**, *33*, 322–335. [CrossRef]
11. Deepika, S.; Sutar, P.P. Spectral selective infrared heating of food components based on optical characteristics and penetration depth: A critical review. *Crit. Rev. Food Sci. Nutr.* **2023**, 1–23. [CrossRef]
12. Shi, X.; Yang, Y.; Li, Z.; Wang, X.; Liu, Y. Moisture transfer and microstructure change of banana slices during contact ultrasound strengthened far-infrared radiation drying. *Innov. Food Sci. Emerg. Technol.* **2020**, *66*, 102537. [CrossRef]
13. Wu, X.; Zhang, M.; Bhandari, B.R. A novel infrared freeze drying (IRFD) technology to lower the energy consumption and keep the quality of *Cordyceps militaris*. *Innov. Food Sci. Emerg. Technol.* **2019**, *54*, 34–42. [CrossRef]
14. Mitrevski, V.; Dedinac, A.; Mitrevska, C.; Bundalevski, S.; Geramitcioski, T.; Mijakovski, V. Mathematical modelling of far-infrared vacuum drying of apple slices. *Therm. Sci.* **2019**, *23*, 393–400. [CrossRef]
15. Salehi, F.; Kashaninejad, M. Modeling of moisture loss kinetics and color changes in the surface of lemon slice during the combined infrared-vacuum drying. *Inf. Process. Agric.* **2018**, *5*, 516–523. [CrossRef]
16. Xi, H.; Liu, Y.; Guo, L.; Hu, R. Effect of ultrasonic power on drying process and quality properties of far-infrared radiation drying on potato slices. *Food Sci. Biotechnol.* **2019**, *29*, 93–101. [CrossRef] [PubMed]
17. Schössler, K.; Henry, J.; Dietrich, K. Effect of continuous and intermittent ultrasound on drying time and effective diffusivity during convective drying of apple and red bell pepper. *J. Food Eng.* **2012**, *108*, 103–110. [CrossRef]
18. Azoubel, P.M.; Baima, M.D.; Amorim, M.D.; Oliveira, S.S. Effect of ultrasound on banana cv Pacovan drying kinetics. *J. Food Eng.* **2010**, *97*, 194–198. [CrossRef]

19. Gamboa-Santos, J.; Montilla, A.; Cárcel, J.A.; Villamiel, M.; García-Pérez, J.V. Air-borne ultrasound application in the convective drying of strawberry. *J. Food Eng.* **2014**, *128*, 132–139. [CrossRef]
20. Feng, Z.; Zhang, M.; Guo, L.; Shao, R.; Wang, X.; Liu, F. Effect of Direct-Contact Ultrasonic and Far Infrared Combined Drying on the Drying Characteristics and Quality of Ginger. *Processes* **2024**, *12*, 98. [CrossRef]
21. Yang, Y.; Zhong, J.; Ma, X.; Li, F.; Fan, X.; Liu, Y. Effect of ultrasonic power on moisture migration and microstructure of contact ultrasound enhanced far-infrared radiation drying on taro slices. *Dry. Technol.* **2023**, *41*, 2189–2200. [CrossRef]
22. Jiang, C.; Wan, F.; Zang, Z.; Zhang, Q.; Xu, Y.; Huang, X. Influence of far-infrared vacuum drying on drying kinetics and quality characteristics of Cistanche slices. *J. Food Process. Preserv.* **2022**, *46*, e17144. [CrossRef]
23. Chinese National Pharmacopoeia Commission. *Chinese Pharmacopoeia*, 1st ed.; China Medical Science and Technology Press: Beijing, China, 2020; pp. 135–136.
24. Beato, V.M.; Orgaz, F.; Mansilla, F.; Montaño, A. Changes in Phenolic Compounds in Garlic (*Allium sativum* L.). *Owing Cultiv. Locat. Growth. Plant Foods Hum. Nutr.* **2011**, *66*, 218–223. [CrossRef]
25. Lay, M.M.; Karsani, S.A.; Mohajer, S.; Abd Malek, S.N. Phytochemical constituents, nutritional values, phenolics, flavonols, flavonoids, antioxidant and cytotoxicity studies on *Phaleria macrocarpa* (Scheff.) Boerl fruits. *BMC Complement. Altern. Med.* **2014**, *14*, 152. [CrossRef] [PubMed]
26. DuBois, M.; Gilles, K.A.; Hamilton, J.K.; Rebers, P.T.; Smith, F. Colorimetric Method for Determination of Sugars and Related Substances. *Anal. Chem.* **1956**, *28*, 350–356. [CrossRef]
27. Nencini, C.; Menchiari, A.; Franchi, G.G.; Micheli, L. In vitro Antioxidant Activity of Aged Extracts of some Italian Allium Species. *Plant Foods Hum. Nutr.* **2011**, *66*, 11–16. [CrossRef] [PubMed]
28. Yao, Z.; Le Maguer, M. Mathematical modeling and simulation of mass transfer in osmotic dehydration process. *J. Food Eng.* **1997**, *32*, 33–46. [CrossRef]
29. Liu, Y.; Zeng, Y.; Hu, X.; Sun, X. Effect of Ultrasonic Power on Water Removal Kinetics and Moisture Migration of Kiwifruit Slices During Contact Ultrasound Intensified Heat Pump Drying. *Food Bioprocess Technol.* **2020**, *13*, 430–441. [CrossRef]
30. Zhang, Y.; Abatzoglou, N. Review: Fundamentals, applications and potentials of ultrasound-assisted drying. *Chem. Eng. Res. Des.* **2020**, *154*, 21–46. [CrossRef]
31. Liu, Y.; Sun, Y.; Yu, H.; Yin, Y.; Li, X.P.; Duan, X. Hot air drying of purple-fleshed sweet potato with contact ultrasound assistance. *Dry. Technol.* **2017**, *35*, 564–576. [CrossRef]
32. Chemat, F.; Rombaut, N.; Sicaire, A.; Meullemiestre, A.; Fabiano-Tixier, A.; Abert-Vian, M. Ultrasound assisted extraction of food and natural products. Mechanisms, techniques, combinations, protocols and applications. A review. *Ultrason. Sonochem.* **2017**, *34*, 540–560. [CrossRef]
33. Sabarez, H.T.; Gallego-Juárez, J.A.; Riera, E. Ultrasonic-Assisted Convective Drying of Apple Slices. *Dry. Technol.* **2012**, *30*, 989–997. [CrossRef]
34. Zhang, Q.; Wan, F.; Zang, Z.; Jiang, C.; Xu, Y.; Huang, X. Effect of ultrasonic far-infrared synergistic drying on the characteristics and qualities of wolfberry (*Lycium barbarum* L.). *Ultrason. Sonochem.* **2022**, *89*, 106134. [CrossRef] [PubMed]
35. Wu, B.; Guo, X.; Guo, Y.; Ma, H.; Zhou, C. Enhancing jackfruit infrared drying by combining ultrasound treatments: Effect on drying characteristics, quality properties and microstructure. *Food Chem.* **2021**, *358*, 129845. [CrossRef] [PubMed]
36. Yao, L.; Fan, L.; Duan, Z. Effect of different pretreatments followed by hot-air and far-infrared drying on the bioactive compounds, physicochemical property and microstructure of mango slices. *Food Chem.* **2020**, *305*, 125477. [CrossRef] [PubMed]
37. Zhao, Y.; Zhu, H.; Xu, J.; Zhuang, W.; Zheng, B.; Lo, Y.M.; Huang, Z.; Tian, Y. Microwave vxacuum drying of lotus (*Nelumbo nucifera Gaertn.*) seeds: Effects of ultrasonic pretreatment on color, antioxidant activity, and rehydration capacity. *Lwt Food Sci. Technol.* **2021**, *149*, 111603. [CrossRef]
38. Pei, Y.; Li, Z.; Xu, W.; Song, C.; Li, J.; Feihu, S. Effects of ultrasound pretreatment followed by far-infrared drying on physicochemical properties, antioxidant activity and aroma compounds of saffron (*Crocus sativus* L.). *Food Biosci.* **2021**, *42*, 101186. [CrossRef]
39. Sun, Y.; Liu, Y.; YU, H.; LI, X. Drying Characteristics and Process Simulation of Ultrasound-Assisted Hot Air Drying of Purple-Fleshed Sweet Potato Based on Weibull Distribution Model. *Food Sci.* **2017**, *7*, 129–135. [CrossRef]
40. Horszwald, A.; Julien, H.; Andlauer, W. Characterisation of Aronia powders obtained by different drying processes. *Food Chem.* **2013**, *141*, 2858–2863. [CrossRef]
41. Qi, Z.Q. Study on microwave-vacuum drying of *Lycium barbarum* polysaccharide extracts and analysis of its quality. *Sci. Technol. Food Ind.* **2013**, *23*, 266–270.
42. Wang, W.; Wu, X.; Chantapakul, T.; Wang, D.; Zhang, S.; Ma, X.; Ding, T.; Ye, X.; Liu, D. Acoustic cavitation assisted extraction of pectin from waste grapefruit peels: A green two-stage approach and its general mechanism. *Food Res. Int.* **2017**, *102*, 101–110. [CrossRef] [PubMed]
43. Jiang, C.; Wan, F.; Zang, Z.; Zhang, Q.; Ma, G.; Huang, X. Effect of an Ultrasound Pre-Treatment on the Characteristics and Quality of Far-Infrared Vacuum Drying with Cistanche Slices. *Foods* **2022**, *11*, 866. [CrossRef] [PubMed]
44. Chen, Z.; Wang, C.; Ma, H.; Ma, Y.; Yan, J. Physicochemical and functional characteristics of polysaccharides from okra extracted by using ultrasound at different frequencies. *Food Chem.* **2021**, *361*, 130138. [CrossRef]
45. Niwa, Y.; Kanoh, T.; Kasama, T.; Negishi, M. Activation of antioxidant activity in natural medicinal products by heating, brewing and lipophilization. A new drug delivery system. *Drugs Under Exp. Clin. Res.* **1988**, *14*, 361–372.

46. Gabriel, A.A. Inactivation behaviors of foodborne microorganisms in multi-frequency power ultrasound-treated orange juice. *Food Control* **2014**, *46*, 189–196. [CrossRef]
47. Lu, J.; Li, J.; Jin, R.; Li, S.; Yi, J.; Huang, J. Extraction and characterization of pectin from *Premna microphylla* Turcz leaves. *Int. J. Biol. Macromol.* **2019**, *131*, 323–328. [CrossRef] [PubMed]
48. Cuvelier, M.E.; Richard, H.; Berset, C. Comparison of the Antioxidative Activity of Some Acid-phenols: Structure-Activity Relationship. *Biosci. Biotechnol. Biochem.* **1992**, *56*, 324–325. [CrossRef]
49. Tekin, Z.; Başlar, M. The effect of ultrasound-assisted vacuum drying on the drying rate and quality of red peppers. *J. Therm. Anal. Calorim.* **2018**, *132*, 1131–1143. [CrossRef]
50. Jiang, L.; Zhou, B.; Wang, X.; Bi, Y.; Guo, W.; Wang, J.; Yao, R.; Li, M. The Quality Monitoring of Cistanches Herba (*Cistanche deserticola* Ma): A Value Chain Perspective. *Front. Pharmacol.* **2021**, *12*, 782962. [CrossRef]
51. Cai, H.; Bao, Z.; Jiang, Y.; Wang, X.; Fan, X.; Aierken; Maitirouzi, T.P. Qualification of active constituents in *Cistanche tubulosa* from various habitats. *Chin. Tradit. Herb. Drugs* **2007**, *38*, 452–455.
52. Cai, H.; Bao, Z.; Jiang, Y.; Sun, Y.; Xu, X.; Tu, P. Quantitative analysis of three active constituents in crude drug of *Cistanche deserticola* influenced by different factors. *Chin. Tradit. Herb. Drugs* **2013**, *44*, 3223–3230.
53. Liu, Z.; Chao, Z.; Liu, Y.; Song, Z.; Lu, A. Maillard reaction involved in the steaming process of the root of *Polygonum multiflorum*. *Planta Medica* **2009**, *75*, 84–88. [CrossRef] [PubMed]
54. Xu, B.; Feng, M.; Tiliwa, E.S.; Yan, W.; Wei, B.; Zhou, C.; Ma, H.; Wang, B.; Chang, L. Multi-frequency power ultrasound green extraction of polyphenols from Pingyin rose: Optimization using the response surface methodology and exploration of the underlying mechanism. *LWT* **2022**, *156*, 113037. [CrossRef]
55. Xiao, H.; Bai, J.; Xie, L.; Sun, D.; Gao, Z. Thin-layer air impingement drying enhances drying rate of American ginseng (*Panax quinquefolium* L.) slices with quality attributes considered. *Food Bioprod. Process.* **2015**, *94*, 581–591. [CrossRef]
56. Saengrayap, R.; Tansakul, A.; Mittal, G.S. Effect of far-infrared radiation assisted microwave-vacuum drying on drying characteristics and quality of red chilli. *J. Food Sci. Technol.* **2015**, *52*, 2610–2621. [CrossRef] [PubMed]
57. Ai, Z.; Lin, Y.; Xie, Y.; Mowafy, S.G.; Zhang, Y.; Li, M.; Liu, Y. Effect of High-Humidity Hot Air Impingement Steaming on *Cistanche deserticola* Slices: Drying Characteristics, Weight Loss, Microstructure, Color, and Active Components. *Front. Nutr.* **2022**, *9*, 824822. [CrossRef]
58. Aydoğdu, A.; Sumnu, G.; Sahin, S. Effects of Microwave-Infrared Combination Drying on Quality of Eggplants. *Food Bioprocess Technol.* **2015**, *8*, 1198–1210. [CrossRef]


**Disclaimer/Publisher's Note:** The statements, opinions and data contained in all publications are solely those of the individual author(s) and contributor(s) and not of MDPI and/or the editor(s). MDPI and/or the editor(s) disclaim responsibility for any injury to people or property resulting from any ideas, methods, instructions or products referred to in the content.